Biochemical and Biophysical Research Communications 389 (2009) 612–615

Contents lists available at ScienceDirect

Biochemical and Biophysical Research Communications

journal homepage: www.elsevier.com/locate/ybbrc

Characterization of the Atg17–Atg29–Atg31 complex specifically required for starvation-induced autophagy in *Saccharomyces cerevisiae* ☆

Yukiko Kabeya [a,1], Nobuo N. Noda [b], Yuko Fujioka [b], Kuninori Suzuki [a], Fuyuhiko Inagaki [b], Yoshinori Ohsumi [a,*]

[a] Advanced Research Organization, Integrated Research Institute, Tokyo Institute of Technology, 4259 Nagatsuta-cho, Midori-ku, Yokohama 226-8503, Japan
[b] Department of Structural Biology, Graduate School of Pharmaceutical Sciences, Hokkaido University, N-21, W-11, Kita-ku, Sapporo 001-0021, Japan

ARTICLE INFO

Article history:
Received 4 September 2009
Available online 13 September 2009

Keywords:
Autophagy
Starvation
ATG
Autophagosome
PAS
Rapamycin

ABSTRACT

Nutrient starvation induces autophagy to degrade cytoplasmic materials in the vacuole/lysosomes. In the yeast, *Saccharomyces cerevisiae*, Atg17, Atg29, and Atg31/Cis1 are specifically required for autophagosome formation by acting as a scaffold complex essential for pre-autophagosomal structure (PAS) organization. Here, we show that these proteins constitutively form an Atg17–Atg29–Atg31 ternary complex, in which phosphorylated Atg31 is included. Reconstitution analysis of the ternary complex in *E. coli* indicates that the three proteins are included in equimolar amounts in the complex. The molecular mass of a monomeric Atg17–Atg29–Atg31 complex is calculated at 97 kDa; however, analytical ultracentrifugation shows that the molecular mass of the ternary complex is 198 kDa, suggesting a dimeric complex. We propose that this ternary complex acts as a functional unit for autophagosome formation.

Macroautophagy (autophagy) is an intracellular bulk degradation system [1]. This phenomenon is ubiquitously conserved from yeast to higher eukaryotes. Upon nutrient starvation, cytoplasmic materials are sequestered in autophagosomes for degradation in the lysosome/vacuole. At least 18 autophagy-related (Atg) proteins are localized to the pre-autophagosomal structure (PAS) and participate in autophagosome formation [2,3]. In response to nutrient starvation, the Atg1-Atg13 complex [4] and autophagy-specific Atg proteins (Atg17, Atg29, and Atg31) associate and assemble at the PAS [5]. In contrast to the Atg1-Atg13 complex, the behavior of Atg17, Atg29, and Atg31 proteins remains to be elucidated.

In this study, we characterize Atg17, Atg29, and Atg31, and show that these proteins constitute a stable ternary complex. We reconstitute this ternary complex in *E. coli*, and determine its precise molecular mass by analytical ultracentrifugation.

Materials and methods

Yeast strains and media. BY4741 (*MAT***a** *his3*Δ *leu2*Δ *met15*Δ *ura3*Δ) (ResGen), YKY61 (BY4741 *atg31::ATG31–13Myc-kanMX*) [6], YKY69 (YKY61 *atg17*Δ*::HIS3*), YKY71 (YKY61 *atg29*Δ*::natMX*), and YKY88 (BY4741 *atg17*Δ*::kanMX atg31*Δ*::natMX*) were used in this study. The other *atg* disruptants listed in Fig. 2B were purchased from ResGen. Media and methods for gene disruption have been described previously [7,8].

Plasmids. To obtain p*ATG31*, a 1.6-kb fragment containing the entire *ATG31* gene was cloned from yeast genomic DNA into pRS426 [9]. For expression of Atg31 under the *CUP1* promoter, the open reading frame of *ATG31* was cloned into pYEX-BX (Clontech).

Antibodies. An antibody against recombinant Atg31 was raised against Atg31 fused to glutathione S-transferase (GST), and was affinity purified. Antibodies against Atg1 [10], Atg17 [7], Atg29 [11], and Pgk1 [12] have been described previously. Mouse monoclonal anti-Myc epitope antibody 9E10 and anti-FLAG tag antibody M2 were purchased from Covance Research Products and Sigma, respectively.

Preparation, analytical gel-filtration and ultracentrifugation of recombinant proteins. GST-tagged Atg17, Atg29, and hexa-histidine (His_6)-tagged Atg31 were co-expressed in *E. coli* on pGEX6p vector (GE Healthcare) for Atg17 and pACYCDuet™-1 vector (Novagen) for Atg29 and Atg31. Lysate from co-expressing cells was applied to a glutathione-Sepharose 4B column (GE Healthcare) and the

Abbreviations: ATG genes, autophagy-related genes; PAS, pre-autophagosomal structure

☆ This work was supported in part by grants-in-aid for Scientific Research from the Ministry of Education, Culture, Sports, Science and Technology of Japan.

* Corresponding author. Fax: +81 45 924 5121.
E-mail address: yohsumi@iri.titech.ac.jp (Y. Ohsumi).
[1] Present address: Division of Evolutionary Biology, National Institute for Basic Biology, 38 Nishigonaka, Myodaiji-cho, Okazaki 444-8585, Japan.

0006-291X/$ - see front matter © 2009 Elsevier Inc. All rights reserved.
doi:10.1016/j.bbrc.2009.09.034

GST–Atg17–Atg29–Atg31 complex was eluted with 10 mM glutathione. After cleaving the GST tag from Atg17 with PreScission protease (GE Healthcare), the Atg17–Atg29–His_6–Atg31 complex was applied to a Ni–NTA column (QIAGEN) and eluted with 200 mM imidazole. Further purification of the Atg17–Atg29–Atg31 complex was performed using a prep grade Superdex 200 column (GE Healthcare). Analytical gel filtration chromatography was performed using a Superdex 200 10/300 GL column (GE Healthcare) equilibrated with 20 mM Tris–HCl buffer pH 8.0 and 150 mM NaCl. One-hundred microliters of the Atg17–Atg29–Atg31 complex (2.0 mg/ml) were applied to the column and eluted with the equilibration buffer. Absorbance at 280 nm was used to detect proteins. Each fraction was subjected to SDS–PAGE and proteins were stained with Coomassie Brilliant Blue (CBB). Sedimentation equilibrium experiments were carried out using an XL-I analytical ultracentrifuge (Beckman Coulter, Inc.) with an An-60 Ti rotor at 298 K. 0.2, 0.35, and 0.7 mg/ml of the Atg17–Atg29–Atg31 complex were loaded and data were collected at equilibrium for two different angular velocities: 6000 and 8000 rpm. Data analysis was carried out using the XL-A/XL-I software, version 6.03 (Beckman Coulter, Inc.) based on the Origin software (Microcal, Inc.).

Other methods. Other methods were described previously [7,13]. For phosphatase treatment, proteins extracted by alkaline treatment were precipitated with 10% trichloroacetic acid and treated with 400 U of lambda protein phosphatase (NEB) for 30 min at 30 °C according to the manufacturers' instructions.

Results and discussion

Atg17, Atg29, and Atg31/Cis1 form a stable complex in the cytosol

Recently, Atg29 and Atg31/Cis1 have been individually reported to interact with Atg17 [6,11]. We thus examined the behavior of Atg17, Atg29, and Atg31 *in vivo*. Fractionation analysis of wild-type cells under growth conditions showed that the majority of Atg17, Atg29, and Atg31 were present in the cytosolic fraction (data not shown). This fraction was subjected to gel filtration analysis using a Superdex 200 column. Atg17 eluted mainly in a single peak in fractions corresponding to ~600 kDa ([7] and Fig. 1A). Atg29 eluted in two peaks, the larger of which overlapped with Atg17 (Fig. 1A, fractions #2–4). Most of the Atg31 also fractionated in the ~600 kDa fractions, together with Atg17 and Atg29 (Fig. 1A, fractions #2–4). Coelution of Atg17, Atg29, and Atg31 suggests that these three proteins form a complex of ~600 kDa. The elution patterns of Atg17, Atg29, and Atg31 in rapamycin-treated cells were similar to those in cells grown in nutrient-rich conditions (Fig. 1A), and nitrogen starvation did not affect the elution patterns (data not shown).

Next, we examined physical interactions between Atg17, Atg29, and Atg31 by immunoprecipitation analysis. Atg29 and Atg31 were coprecipitated with Atg17 in a rapamycin-independent manner

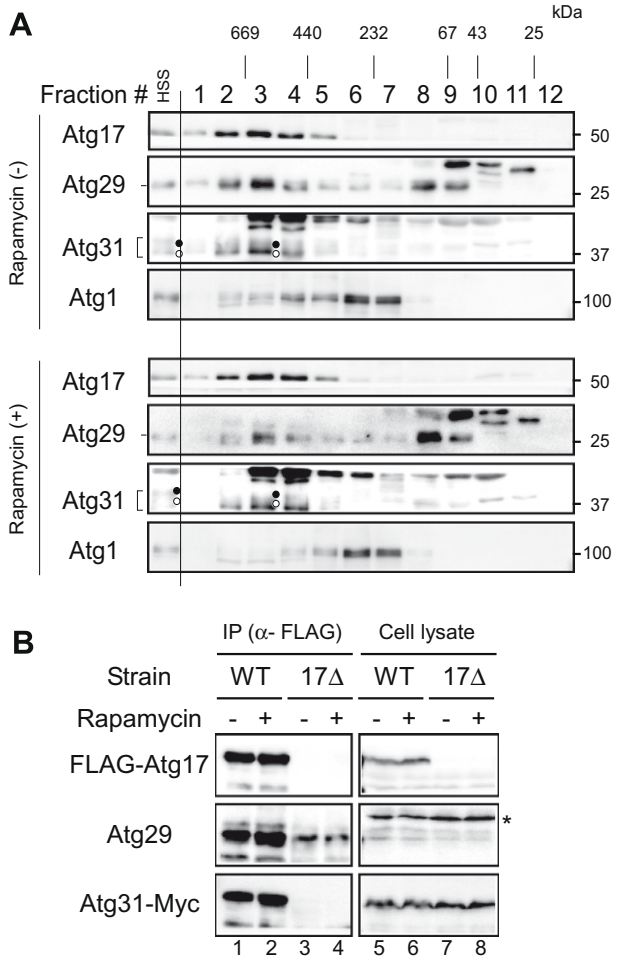

Fig. 1. Atg17, Atg29, and Atg31 form a stable complex *in vivo*. (A) Wild-type cells (BY4741) were grown and treated with rapamycin for 1 h. After cells were converted to spheroplasts, cell lysates were prepared by osmotic lysis. Cytosolic fractions (100,000*g* supernatant) were separated by gel filtration chromatography on a Superdex 200 column. Each fraction was analyzed by immunoblotting using anti-Atg1, anti-Atg17, anti-Atg29, and anti-Atg31antibodies. Positions of molecular mass standards (in kDa) are shown. Open and closed circles indicate dephosphorylated and phosphorylated Atg31, respectively (see the text). (B) *atg17*Δ cells (YKY69) harboring a pFLAG-Atg17 CEN plasmid were grown and treated with rapamycin. FLAG-Atg17 was immunoprecipitated with a monoclonal anti-FLAG antibody and immunoblotted with a polyclonal anti-FLAG antibody. Associated proteins were visualized by immunoblotting with anti-Atg29 and anti-Myc antibodies. The asterisks in the total cell lysates show nonspecific bands that were recognized by the anti-Atg29 antibody.

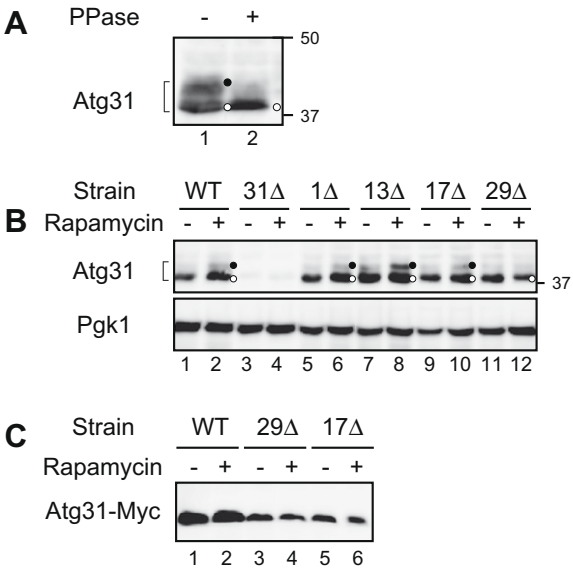

Fig. 2. Atg31 is a phosphoprotein. (A) Lysates from *atg31*Δ cells (BY4741 background) overexpressing Atg31 from the *CUP1* promoter and grown overnight were subjected to phosphatase treatment. After the reaction was terminated by boiling in SDS-sample buffer, samples were subjected to immunoblot with anti-Atg31 antibody. Open and closed circles indicate dephosphorylated and phosphorylated forms of Atg31, respectively. (B) Wild-type cells and each *atg* disruptant (BY4741 background) were treated with rapamycin for 1 h. The lysates were subjected to immunoblot using anti-Atg31 antibody. Pgk1 served as a loading control. (C) Wild-type (YKY61), *atg17*Δ (YKY69), and *atg29*Δ (YKY71) cells chromosomally expressing Atg31-Myc were treated with rapamycin for 1 h. Total lysates were subjected to immunoblot with an anti-Myc antibody.

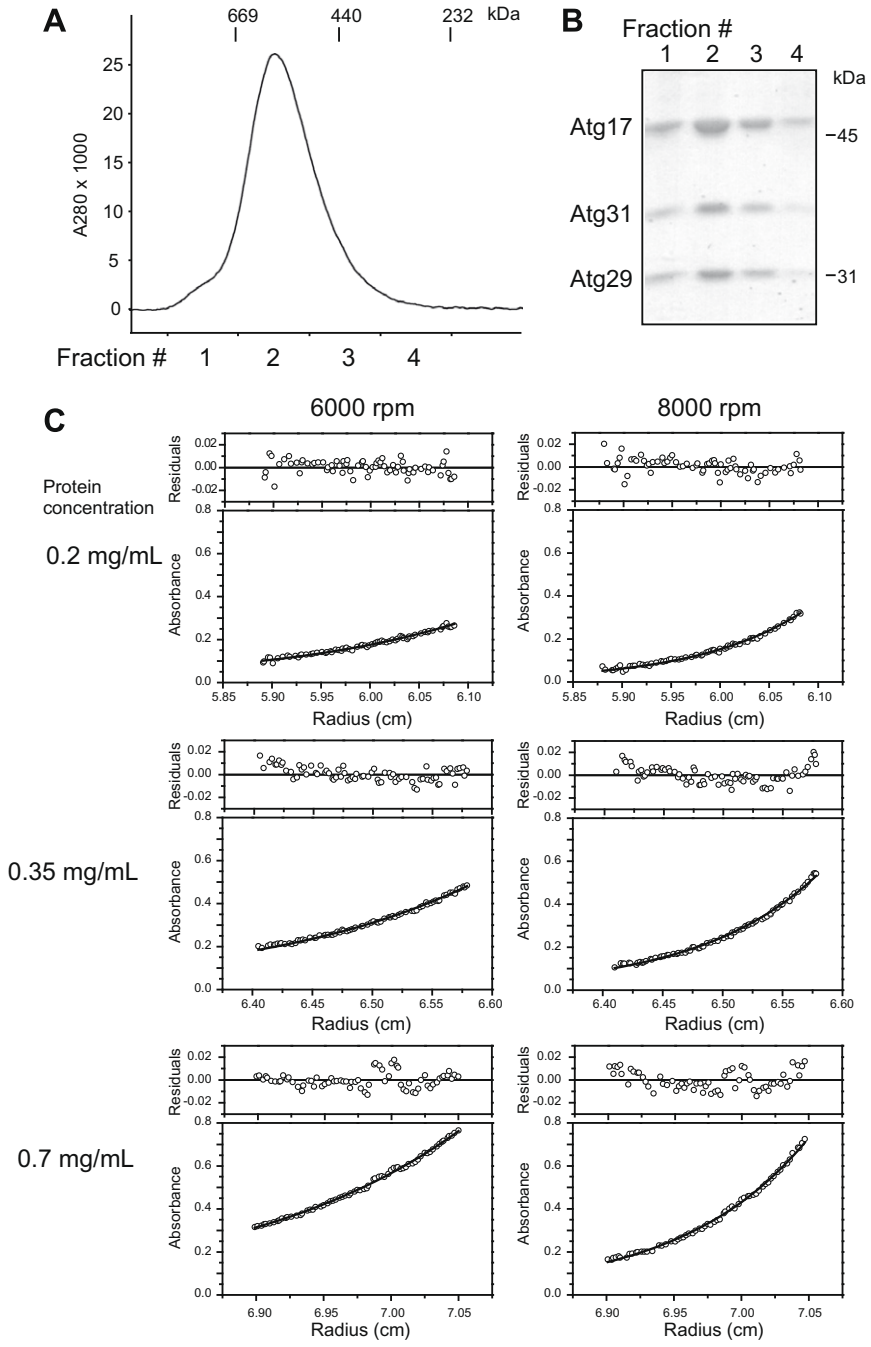

Fig. 3. Reconstitution of the Atg17–Atg29–Atg31 complex in *E. coli*. (A) Heterotrimeric Atg17–Atg29–Atg31 complex was subjected to gel filtration chromatography on a Superdex 200 column and the resulting elution profile is shown. (B) The proteins in each fraction were separated by SDS–PAGE and stained with CBB. (C) Sedimentation equilibrium profiles for the reconstituted Atg17–Atg29–Atg31 complex at initial loading concentrations of 0.2 (top), 0.35 (middle), and 0.7 mg/ml (bottom). Samples in 20 mM Tris–HCl buffer at pH 8.0 and 150 mM NaCl were centrifuged at 298 K for 20 h at 6000 and 8000 rpm. Absorbances at 280 nm at sedimentation equilibrium (*left*, 6000 rpm; *right*, 8000 rpm) are shown as a function of the radial cell position from the axis of rotation. Nonlinear least squares fits to a model that assumes a single ideal species are overlaid onto these data sets. Residuals for the nonlinear least square fits are plotted versus the distance from the axis of rotation above each graph. Global fitting yielded an apparent average molecular mass of 197,601 Da for the Atg17–Atg29–Atg31 complex.

(Fig. 1B). This result shows that the Atg17–Atg29–Atg31 complex is stable, and is formed constitutively and independent of nutrient conditions.

We reported that the association of the Atg1-Atg13 complex with Atg17, Atg29, and Atg31 is markedly enhanced in response to nutrient starvation, and that these five proteins act as a scaffold that stimulates the recruitment of the other Atg proteins to the PAS [5]. In gel filtration analysis using rapamycin-treated cells, Atg1 and Atg13 were mainly eluted in smaller fractions (Fig. 1A, fractions #6–7; data not shown) than the Atg17–Atg29–Atg31 complex (Fig. 1A, fractions #2–4), indicating that most of the Atg1 and Atg13 do not form a stable complex with the Atg17–Atg29–Atg31 complex. In fact, in the absence of Atg1 or Atg13, the ~600 kDa Atg17–Atg29–Atg31 complex was normally detected by gel filtration analysis and, conversely, the elution patterns of Atg1 and Atg13 did not change in *atg17*Δ, *atg29*Δ or *atg31*Δ cells (data not shown). Although gel filtration analysis showed that the main peaks of Atg1 (or Atg13) and the Atg17–Atg29–Atg31

complex are different, it is still possible that a very small population of Atg1 and Atg13 interacts with the Atg17–Atg29–Atg31 complex in response to starvation, which might be sufficient to induce autophagosome formation. Alternatively, the interaction between Atg1 and the Atg17–Atg29–Atg31 complex may not be strong enough to be analyzed under our experimental conditions.

Atg31 is a phosphoprotein

Atg31 was recognized as two bands at ~40 kDa by immunoblot analysis and the upper band disappeared following phosphatase treatment (Fig. 2A), indicating that Atg31 is phosphorylated. Phosphorylated Atg31 was detectable in the Atg17–Atg29–Atg31 complex in cells under both growth and rapamycin-treated conditions (Fig. 1A). The expression of Atg31 was upregulated by nitrogen depletion or addition of rapamycin [14], resulting in an increase of phosphorylated Atg31 (Fig. 2B, lanes 1–2). We examined the phosphorylation level of Atg31 in several *atg* mutants. Atg1 is a protein kinase essential for autophagy, and its kinase activity is regulated by binding to Atg13 [4,10]. However, the phosphorylation levels of Atg31 in *atg1*Δ and *atg13*Δ cells were not decreased (Fig. 2B, lanes 5–8), suggesting that Atg1 and Atg13 are not involved in phosphorylation of Atg31. The amount of Atg31 was decreased in *atg17*Δ or *atg29*Δ cells (Fig. 2C). This result suggests that the absence of Atg17 or Atg29 makes Atg31 unstable, resulting in a decrease of phosphorylated Atg31.

Atg17, Atg29, and Atg31 form a stoichiometric complex

We next examined whether Atg17, Atg29, and Atg31 are able to constitute a complex. GST–Atg17, Atg29, and His_6–Atg31 were co-expressed in *E. coli*, and proteins associating with both Atg17 and Atg31 were purified using a glutathione column and a Ni-chelating column. Gel filtration analysis showed that the purified Atg17 complex was collected at fractions of ~600 kDa (Fig. 3A). SDS–PAGE followed by CBB staining demonstrated that Atg29 and Atg31 were co-eluted in this fraction (Fig. 3B, fraction #2), indicating that Atg17, Atg29, and Atg31 form a ~600 kDa complex in *E. coli*. The amounts of Atg17 and Atg29 relative to Atg31 were estimated by densitometry; the ratio of Atg17, Atg29, and Atg31 was about 2:1:1, which corresponds to that of the theoretical molecular masses of Atg17, Atg29, and Atg31 (49 kDa:25 kDa:23 kDa = 2.13:1.09:1.00). We conclude that an equal number of Atg17, Atg29, and Atg31 was included in the reconstituted complex; further, the molecular mass of the monomeric Atg17–Atg29–Atg31 complex was calculated at 97 kDa.

As the molecular mass estimated by gel filtration analysis is affected by the shape of a protein complex, we used equilibrium analytical ultracentrifugation to determine a more accurate size. This experiment provided a molecular mass of 198 kDa for the Atg17–Atg29–Atg31 complex (Fig. 3C), indicating the complex is likely dimeric. This apparent size is much smaller than that deduced from the gel filtration chromatography (~600 kDa); the inconsistency may be due to a non-globular shape of the Atg17–Atg29–Atg31 complex. Structural analysis of the Atg17–Atg29–Atg31 complex will solve this problem.

Here, we characterized the Atg17–Atg29–Atg31 complex biochemically. Atg17, Atg29, and Atg31 form a stable complex independent of nutrient conditions (Figs. 1 and 2). Moreover, we reconstituted the Atg17–Atg29–Atg31 complex in *E. coli*, and determined its molecular mass to be 198 kDa (Fig. 3).

At present, a homolog of Atg31 has been identified only in *Candida glabrata* (CAG61687), but not in higher eukaryotes. Using a gapped BLAST search, Meijer et al. identified putative orthologs of yeast Atg17 and Atg29 in *Schizosaccharomyces pombe* (CAA15724) and *Gibberella zeae* (EAA77407), respectively [15]. Recently, in mammalian cells, FIP200 has been found to share several features with yeast Atg17, even though little similarity is found in their amino acid sequences [16]. In addition, Atg101 has been identified in mammals. Atg101 interacts with ULK1, the mammalian homolog of Atg1, via Atg13 [17]. Further analysis of functional counterparts of Atg17, Atg29, and Atg31 in higher eukaryotic cells may help to elucidate the mechanisms of regulation of autophagy upon starvation.

Acknowledgments

We thank H. Nakatogawa (in our laboratory) for helpful discussion and the National Institute for Basic Biology Center for Analytical Instruments for technical assistance.

References

[1] H. Nakatogawa, K. Suzuki, Y. Kamada, Y. Ohsumi, Dynamics and diversity in autophagy mechanisms: lessons from yeast, Nat. Rev. Mol. Cell Biol. 10 (2009) 458–467.
[2] K. Suzuki, T. Kirisako, Y. Kamada, N. Mizushima, T. Noda, Y. Ohsumi, The pre-autophagosomal structure organized by concerted functions of *APG* genes is essential for autophagosome formation, EMBO J. 20 (2001) 5971–5981.
[3] K. Suzuki, Y. Kubota, T. Sekito, Y. Ohsumi, Hierarchy of Atg proteins in pre-autophagosomal structure organization, Genes Cells 12 (2007) 209–218.
[4] Y. Kamada, T. Funakoshi, T. Shintani, K. Nagano, M. Ohsumi, Y. Ohsumi, Tor-mediated induction of autophagy via an Apg1 protein kinase complex, J. Cell Biol. (2000) 1507–1513.
[5] T. Kawamata, Y. Kamada, Y. Kabeya, T. Sekito, Y. Ohsumi, Organization of the pre-autophagosomal structure responsible for autophagosome formation, Mol. Biol. Cell 19 (2008) 2039–2950.
[6] Y. Kabeya, T. Kawamata, K. Suzuki, Y. Ohsumi, Cis1/Atg31 is required for autophagosome formation in *Saccharomyces cerevisiae*, Biochem. Biophys. Res. Commun. 356 (2007) 405–410.
[7] Y. Kabeya, Y. Kamada, M. Baba, H. Takikawa, M. Sasaki, Y. Ohsumi, Atg17 functions in cooperation with Atg1 and Atg13 in yeast autophagy, Mol. Biol. Cell 16 (2005) 2544–2553.
[8] A.L. Goldstein, J.H. McCusker, Three new dominant drug resistance cassettes for gene disruption in *Saccharomyces cerevisiae*, Yeast 15 (1999) 1541–1553.
[9] R.S. Sikorski, P. Hieter, A system of shuttle vectors and yeast host strains designed for efficient manipulation of DNA in *Saccharomyces cerevisiae*, Genetics 122 (1989) 19–27.
[10] A. Matsuura, M. Tsukada, Y. Wada, Y. Ohsumi, Apg1p, a novel protein kinase required for the autophagic process in *Saccharomyces cerevisiae*, Gene 192 (1997) 245–250.
[11] T. Kawamata, Y. Kamada, K. Suzuki, N. Kuboshima, H. Akimatsu, S. Ota, M. Ohsumi, Y. Ohsumi, Characterization of a novel autophagy-specific gene, *ATG29*, Biochem. Biophys. Res. Commun. 338 (2005) 1884–1889.
[12] M. Baba, K. Takeshige, N. Baba, Y. Ohsumi, Ultrastructural analysis of the autophagic process in yeast: Detection of autophagosomes and their characterization, J. Cell Biol. 124 (1994) 903–913.
[13] A. Kuma, N. Mizushima, N. Ishihara, Y. Ohsumi, Formation of the ~350 kD Apg12-Apg5**.** Apg16 multimeric complex, mediated by Apg16 oligomerization, is essential for autophagy in yeast, J. Biol. Chem. 277 (2002) 18619–18625.
[14] A.P. Gasch, P.T. Spellman, C.M. Kao, O. Carmel-Harel, M.B. Eisen, G. Storz, D. Botstein, P.O. Brown, Genomic expression programs in the response of yeast cells to environmental changes, Mol. Biol. Cell 11 (2000) 4241–4257.
[15] W.H. Meijer, I.J. van der Klei, M. Veenhuis, J.A. Kiel, *ATG* genes involved in non-selective autophagy are conserved from yeast to man, but the selective Cvt and pexophagy pathways also require organism-specific genes, Autophagy 3 (2007) 106–116.
[16] T. Hara, A. Takamura, C. Kishi, S. Iemura, T. Natsume, J.L. Guan, N. Mizushima, FIP200, a ULK-interacting protein, is required for autophagosome formation in mammalian cells, J. Cell Biol. 181 (2008) 497–510.
[17] C.A. Mercer, A. Kaliappan, P.B. Dennis, A novel, human Atg13 binding protein, Atg101, interacts with ULK1 and is essential for macroautophagy, Autophagy 5 (2009) 649–662.